City Research Online

City St George's, University of London

Citation: Gkatzogias, K.I. & Kappos, A. J. (2015). Deformation-based seismic design of concrete bridges. Earthquakes and Structures, 9(5), pp. 1045-1067. doi: 10.12989/eas.2015.9.5.1045

This is the accepted version of the paper.

This version of the publication may differ from the final published version. To cite this item please consult the publisher's version.

Permanent repository link: https://openaccess.city.ac.uk/id/eprint/13490/

Link to published version: https://doi.org/10.12989/eas.2015.9.5.1045

Copyright and Reuse: Copyright and Moral Rights remain with the author(s) and/or copyright holders. Copies of full items can be used for personal research or study, educational, or not-for-profit purposes without prior permission or charge, unless otherwise indicated, provided that the authors, title and full bibliographic details are credited, a hyperlink and/or URL is given for the original metadata page and the content is not changed in any way. For full details of reuse please refer to City Research Online policy.

City Research Online: http://openaccess.city.ac.uk/ publications@citystgeorges.ac.uk

Deformation-based seismic design of concrete bridges

Konstantinos I. Gkatzogias*, Andreas J. Kappos[a]

Department of Civil Engineering, City University London, London EC1V 0HB, United Kingdom

(Received , Revised , Accepted)

Abstract. A performance-based design (PBD) procedure, initially proposed for the seismic design of buildings, is tailored herein to the structural configurations commonly adopted in bridges. It aims at the efficient design of bridges for multiple performance levels (PLs), achieving control over a broad range of design parameters (i.e. strains, deformations, ductility factors) most of which are directly estimated at the design stage using advanced analysis tools (a special type of inelastic dynamic analysis). To evaluate the efficiency of the proposed design methodology, it is applied to an actual bridge that was previously designed using a different PBD method, namely displacement-based design accounting for higher mode effects, thus enabling comparison of the alternative PBD approaches. Assessment of the proposed method using nonlinear dynamic analysis for a set of spectrum-compatible motions, indicate that it results in satisfactory performance of the bridge. Comparison with the displacement-based method reveals significant cost reduction, albeit at the expense of increased computational effort.

Keywords: deformation-based design; direct displacement-based design; nonlinear dynamic analysis; bridges; reinforced concrete

1. Introduction

In the quest for a 'new generation' of performance-based codes, that will minimise direct and indirect losses due to earthquakes, several design procedures were developed (*fib* 2003), attempting to reconcile the requirements for simplicity (important in practical design) and enhanced control of the performance of both structural and non-structural members. The inherent difficulties in this attempt along with the preference of each research group for focussing on specific design parameters (typically at the expense of others), resulted in marked differences among the suggested approaches with regard to the adopted design procedures (e.g. type of analysis, definition of seismic input) (Kappos 2015). Until recently, implementation of these concepts to bridges has been quite limited, despite their critical role in the roadway and railway networks and the fact that their vulnerability to earthquakes has long been established, particularly with regard to their post-earthquake 'operationality'.

Notwithstanding the fact that elastic dynamic (response spectrum) analysis remains the most commonly used method in seismic design of both buildings and bridges (e.g. CEN 2005a), there is little doubt that an increasing number of engineers (researchers, but also practitioners) utilise advanced analysis tools to estimate the response of bridge structures (especially when the bridge

*Corresponding author, PhD candidate, E-mail: Konstantinos.Gkatzogias.1@city.ac.uk
[a] Professor, E-mail: Andreas.Kappos.1@city.ac.uk

considered is of high importance) under challenging conditions (i.e. complex structural configuration and increasing size of bridges, site-effects, diversity of actions). The development of a good number of software packages for the inelastic dynamic (response-history) analysis of bridges and other structures is the natural consequence of this trend.

In view of the above, the present study attempts to present a rigorous design methodology for concrete bridges, in a performance-based context; i.e. explicitly designing for multiple PLs based on a procedure wherein the structural characteristics associated with each PL are determined in a non-iterative way. The proposed approach (hereafter referred to as Def-BD) is developed with ductility of piers as a key design parameter, hence, focuses on bridges having their deck connected to one or more piers (as opposed to seismic isolation solutions); nevertheless, deformation capacity of bearings is also among the adopted criteria. It originates from work by the second author and his associates focused on the seismic design of buildings (Kappos 1997, Kappos and Manafpour 2001, Kappos and Panagopoulos 2004, Kappos *et al.* 2007, Kappos and Stefanidou 2010); detailed steps and required modifications presented herein refer to the latest (2010) version of the previous methodology. The efficiency of the proposed design methodology is subsequently assessed by applying it to an actual bridge selected with a view to enabling comparison between the suggested procedure and the direct displacement-based design method (Priestley *et al.* 2007), as extended by Kappos *et al.* (2013) to explicitly account for higher mode effects. Details of the latter methodology (hereafter referred to as MDDBD) regarding the adopted design assumptions (i.e. response spectrum analysis, displacement spectrum, secant stiffness at yield, controlled parameters) and identified limitations can be found elsewhere (Kappos *et al.* 2012, 2013), along with its implementation to the same bridge considering a single PL (i.e. 'life-safety'). The suggested procedure and the resulting designs for two different seismic zones are subsequently evaluated in the light of nonlinear dynamic analysis using a number of spectrum-compatible motions, whereas comparisons between Def-BD and MDDBD are made in terms of both economy and seismic performance.

2. A deformation-based design procedure for bridges

A PBD procedure based on deformation control and involving a special type of nonlinear response history analysis (NLRHA), initially proposed for buildings, is tailored herein to seismic design of bridges. Detailed steps of the procedure are presented, with emphasis on the required modifications and/or extensions that arise from the different structural configuration of bridges (i.e. intended plastic mechanism, estimation of required pier strength and proper detailing) and the possibility to use passive control devices. The suggested deformation-based design procedure, described in the following steps, estimates initially design quantities from empirical relationships (Step 1), while incorporating inelastic analytical tools (section analysis, dynamic analysis) in subsequent steps, leading to a gradual refinement of the final design solution through the control of a wide range of material strains and deformations. It is noted that by duly exercising engineering judgment, a more limited number of deformations can be selected as controlled parameters, which simplifies the procedure.

Step 1 – Flexural design of plastic hinge zones based on 'operationality' criteria: The purpose of this step is to establish a basic level of strength in the structure that would ensure that the bridge remains operational during and after an earthquake having a relatively high probability of

exceedance (frequent earthquake level, denoted as EQII); regarding ordinary bridges, modern codes and guidelines (CEN 2005a, NZTA 2013, ATC/MCEER 2004, FHWA 2006) provide a return period (T_r) within the range of 40 to 110 years, modifying either T_r or the severity of the performance requirements in the case of bridges of higher or lower importance. The 'operationality' verifications adopted herein include specific limits for strains, curvature and rotational ductility factors (see Step 2) and the corresponding demands are estimated from inelastic analysis of a partially inelastic model of the structure (also described in Step 2). Since for any inelastic analysis to be carried out the strength of the yielding zones has to be an input parameter, an initial elastic analysis is required, which would provide the strength of the members (selected energy dissipation zones) that will respond inelastically during the 'operationality' verification; this analysis constitutes Step 1 and is a vital part of the procedure.

The design of selected dissipating zones, like the pier ends, is carried out using conventional elastic analysis (modal response spectrum, or equivalent static, analysis, depending on the importance of higher modes). The strength of these zones is estimated taking into consideration the range within which the inelastic deformations should fall, which corresponds to the degree of damage allowed for the selected PL (more specifically the allowable rotational ductility factor). The procedure described in the following provides an initial estimate of the allowable rotational ductility factor while aiming at the development of permissible values of inelastic deformations under the frequent earthquake event, since the latter are directly related to the reduction of element forces corresponding to elastic behaviour. This is a critical feature, not included in earlier versions of the method (tailored to buildings) that either included a serviceability check, the result of which typically was that most members remained elastic (or were well below the allowable deformation limits) (Kappos and Panagopoulos 2004), or estimated the strength of the dissipating zones by adopting a fixed value for the allowable rotational ductility factor (Kappos and Stefanidou 2010).

To meet the aforementioned objective, element forces and chord rotations are first obtained from the results of a standard response spectrum (elastic) analysis. The pier stiffness considered at this stage is the secant value at yield, accounting for the effects of axial load ratio; the diagrams proposed by Priestley *et al.* (1996) and adopted by Caltrans (2013) can be used, considering the axial load for the seismic combination, and assuming either minimum reinforcement (1%) or that resulting from design for non-seismic loading (if higher than 1%).

Design for flexure is carried out in terms of design values of material strength (in reinforced concrete piers f_{cd} and f_{yd} for concrete and steel, respectively, using Eurocode notation) using commonly available design aids. On the other hand, 'operationality' checks (Step 2) are based on the results of inelastic analysis, for which mean values are commonly adopted (f_{cm} and f_{ym}); furthermore, some members are expected to possess overstrength with respect to the design moments used in their dimensioning, due to detailing requirements, i.e. rounding (upwards) of required reinforcement areas and use of minimum reinforcement specified by codes. For these two reasons, the initial elastic analysis should be carried out for an appropriate fraction (v_0) of the earthquake level associated with the 'operationality' PL. Due to the expected overstrength, the recommended v_0 factor is lower than the ratio f_{yd}/f_{ym} (equal to 0.79 if the mean yield strength of steel f_{ym} is taken as 10% higher than the characteristic strength f_{yk}). Furthermore, the v_0 factor should also account for the differences in the moments derived from a response spectrum analysis (RSA) and those from a series of response history analyses (RHAs) for selected accelerograms (see Step 2). As an alternative, one could opt to use design values of yield moments in the inelastic analysis (a practice not adopted by current codes), in which case a different v_0 factor should be used; note that if v_0=1 is selected piers will not yield under EQII, which is deemed as a very high

PL, justified in economic terms only for critical bridges (ATC/MCEER 2004, FHWA 2006, Caltrans 2014). It is perhaps worth noting that the problem of mixing design and mean values of material strength is by no means specific to the PBD method presented here; modern codes like Eurocode 8 - Part 1 (EC8-1) (CEN 2004b) adopt both elastic and inelastic analysis methods and recommend using design values for strength verifications and mean values for displacement or deformation verifications.

Subsequently, elastic chord rotations (θ_{el}) are related to the corresponding inelastic ones (θ_{inel}), using an empirical procedure like the one proposed by Bardakis and Fardis (2011); use of empirical factors to estimate θ_{inel} is an inherent limitation of the proposed procedure, since otherwise ductility factors cannot be estimated at this stage. The allowable (target) chord rotation ductility factor ($\mu_{\theta,ls}$) for this PL can be estimated from Eq. (1), where the allowable curvature (φ_{ls}), the yield curvature (φ_y) and the plastic hinge length are estimated using empirical equations and diagrams (e.g. Kowalsky 2000, Priestley *et al.* 2007, Biskinis & Fardis 2010, Cardone 2014). The equivalent cantilever height (h_{eq}) (the length from the critical section to the point of contraflexure, i.e. the shear span) of each pier can be approximated from the results of the elastic analysis.

$$\mu_{\theta,ls} = 1 + \theta_{pl,ls} / \theta_y = 1 + 3 \cdot \left(\varphi_{ls} - \varphi_y \right) \cdot L_{pl} / \left(\varphi_y \cdot h_{eq} \right) \quad (1)$$

Referring to Fig. 1(a), having defined $\mu_{\theta,ls}$ and θ_{inel} (this is the total chord rotation, not the plastic one), from the θ_{el} found in the elastic analysis, the yield rotation ($\theta_y = \theta_{inel}/\mu_{\theta,ls}$) is calculated for every pier. For simplicity, one could assume first that M-θ response is elastic-perfectly plastic and second that the slopes of the elastic and the elastoplastic M-θ diagrams are the same. Then the yield moment (M_y) of each pier can be easily computed, as the intersection of the elastic part of the diagram and the vertical line drawn at θ_y, as shown in Fig. 1(a); this is the moment to be used for the (flexural) design of the pier, implicitly related to an earthquake intensity associated with the yield state of the bridge (i.e. lower than EQII), denoted here as EQI. A more accurate procedure for the definition of yield moments in the dissipating zones, accounting for the loading history of the structure (i.e. application of the pertinent combination of permanent and transient actions prior to the application of seismic loads), has been proposed by Kappos and Stefanidou (2010) for the case of buildings (Fig. 1(b)). However, in the case of bridges where the dissipating zones are expected to form in the piers (instead of the beams) this refinement is typically not necessary, since the bending moment induced in the piers by gravity loading is in most cases small compared to that from seismic loading.

The reduced design moments are computed for every pier according to the previous procedure, and they are directly related to the target rotational ductility of Eq. (1). The longitudinal reinforcement demand for the piers is calculated using standard flexural design procedures and compared to code minimum requirements. In case the longitudinal reinforcement demands are found to be less than the minimum requirements, reduction of cross sections is in order (reduction of stiffness), otherwise deformations for the considered PL will be less than the allowable ones, which of course is an option, but does not optimise the cost of the bridge.

In the case of bridges (and in contrast to buildings) deformation control in the piers does not fully guarantee that the bridge will remain operational; it is equally important to check that bearings (which are typically present unless a fully integral solution is adopted) also remain functional. Hence, displacements (or the corresponding strains) of bearings under the full 'operationality' earthquake (i.e. excluding the factor ν_0 and adopting the 'equal-displacement rule at this stage of design) should conform to the deformation criteria discussed in Step 2; clearly, this

stage involves striking a balance between economy and performance.

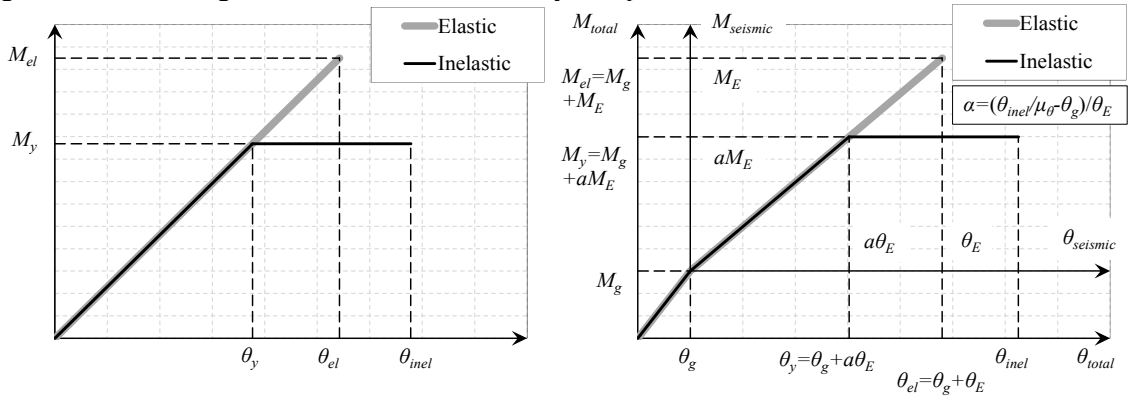

(a) Bilinear (elastoplastic) M-θ approximation (b) Trilinear M-θ approximation

Fig. 1 Definition of pier yield moments

Step 2 – Serviceability/operationality verifications: During this step a partially inelastic model (PIM) of the structure is set up, wherein the energy dissipation zones of the piers (e.g. top and bottom of columns if they are monolithically connected to the deck) are modelled as yielding elements, with their strength based on the reinforcement calculated for reduced column moments according to the inelastic deformations allowed for the 'operationality' limit-state (Step 1). In the same model, the remaining parts of the bridge are modelled as elastic members apart from the case of passive control devices that exhibit a nonlinear behaviour under the considered PL. Since the dissipating zones have been designed for flexure at Step 1, the stiffness of the piers can now be calculated from moment-curvature (M-φ) analysis using the longitudinal reinforcement ratio (ρ_l) of the pier ends and mean values for strength of materials, since deformations are to be checked at this stage.

NLRHA of the PIM also requires the definition of a suite of ground motions compatible with the selected design spectrum. At least seven accelerograms are required according to codes such as EC8-1 if average response quantities are to be used for design. The accelerogram set used for 3D analysis should include a pair of components for every seismic motion, provided the vertical component is not important for the design of the bridge (which is not always the case). The ground motions should be selected on the basis of the results of a seismic hazard analysis ('deaggregation' phase, wherein the 'design' magnitude (M_s) and epicentral distance (R) for the site in consideration are determined). Hence the selected ground motions should conform to certain criteria concerning magnitude (e.g. M_s=6.0~6.5), epicentral distance (e.g. R=10~25km), and peak ground acceleration (e.g. PGA>~0.1g). Additional criteria, not specifically required by EC8, but important all the same, are the similarity of spectra (of the selected motions to the target spectrum) and the reliable estimate of the mean structural response, depending on the accepted variability of critical member responses; software for such multi-criteria selection of the design accelerograms is currently available, e.g. Katsanos and Sextos (2013).

The aforementioned earthquake motions will be used for both this step and the following one, and they should be properly scaled to the level associated with the limit-state considered, i.e. 'operationality' limit-state for the design of energy dissipation zones, and 'life-safety' for the other members. Depending on whether analysis is carried out separately in each direction of the bridge

or simultaneously in both directions a different scaling procedure is in order. For instance in the former case the procedure prescribed by EC8-1 can be used, while in the latter case the procedure of Eurocode 8 - Part 2 (EC8-2) (CEN 2005a) is recommended; the issue is further discussed in the case study presented later. It is noted here that the assumption that the shape of the design spectrum remains the same regardless of the intensity of the earthquake (i.e. the same for T_r=100 and T_r=500) is strictly not valid, but is commonly adopted, also herein, for simplifying the design procedure; of course the procedure is applicable regardless of the degree of sophistication involved in selecting the ground motions, which is also affected by the importance of the bridge.

The verifications for the 'operationality' limit-state can be carried out in terms of specific limits for maximum drifts and plastic deformations of critical members (i.e. the piers). The limits can be derived on the basis of accepted damage, especially in the context of allowing the bridge to remain operational under this level of seismic action. Several criteria are discussed in *fib* (2007) and it is clear that the proposals available in the literature vary substantially, from conservative ones (e.g. Choi *et al.* 2004) addressing columns not designed for seismic actions, to very daring ones (e.g. Priestley *et al.* 1996) intended for modern ductile bridge piers. A more appropriate way to define acceptable damage for R/C piers in line with the refined analysis tools used in the suggested procedure, is in terms of strains; for instance, it is clear that the functionality of the bridge will not be impaired if cover concrete does not spall, which typically occurs at strains between 3.5 and 4‰. Such strain values can then be used to derive limits for deformation (e.g. curvature and/or chord rotation ductility factors) and/or displacement, based on the results of the M-φ analysis of pier columns, and the h_{eq} taken as the mean of the relevant response quantities observed during the nonlinear dynamic analyses. Regarding bearings and in particular the usual type of bolted elastomeric bearings, the deformation limit associated with a functionality level could be set, in terms of bearing strain, between 0.5 and 1.5 (Padgett 2007, Moschonas *et al*. 2009, Cardone 2014). Moreover, the width of joints (in modern bridges normally located solely at the abutments, except for very long decks with intermediate joints) should be selected such that they remain open under this level of seismic action, to avoid damage at the backwalls.

The purpose of this step, apart from checking the overall inelastic performance of the structural system, is the verification that the required deformations in the piers are consistent with the limit-state values calculated in accordance with the section analysis results. If the limit-state deformation criteria are not satisfied (e.g. within 10%), stiffening or softening of the pier columns will be required; modification of ρ_l is more appropriate for deformation control, while the diameter of the pier columns controls effectively drifts and displacements. In this context, this step is basically an assessment (or verification) of the seismic response of the bridge for the 'operationality' level. Since inelastic dynamic analysis is used to check the seismic response of the structure for the aforementioned PL, mean values of material strength are considered (f_{cm} and f_{ym} for concrete and steel, respectively).

Step 3 – Verifications for the 'life-safety' or 'repairable damage' limit-state: The design of members (such as the deck, the abutments, and the foundation) considered elastic in setting up the PIM, is verified on the basis of results of NLRHA of the aforementioned model for each of the selected sets of input motions properly scaled to the intensity of the motion associated with the 'life-safety' requirement or the 'design earthquake' in terms of current code provisions (denoted here as EQIII). The return period associated with this PL varies significantly among different codes; e.g. for ordinary bridges the 'design earthquake' T_r is defined as 475 yrs in EC8-2 (CEN 2005a), 1033 in AASHTO (2011) and FHWA (2006), 2462 in ATC/MCEER (2004), 3000 in NZTA (2013), whereas in Caltrans (2013) the design response spectrum is defined as an envelope

between a deterministic (i.e. a maximum credible event) and a probabilistic spectrum (of T_r=975 yrs). Although a review of the performance criteria adopted by current codes is beyond the scope of this paper, adopting an increased useful life (e.g. 100 yrs) and the same probability of exceedance as in buildings (i.e 10%/100 yrs instead of 10%/50 yrs), yields a return period in the order of 1000 yrs which is in line with the current trend in US codes (but not in EC8-2). In terms of structural performance, it is suggested that this level be selected as the 'repairable damage' limit state, i.e. the extent of damage is such that first it can be repaired after the earthquake (closure of the bridge will be required for a certain period) and second there is no noticeable risk to life.

This is an important step for buildings (Kappos and Stefanidou 2010) since several critical elements, in particular the columns (except at the base of the ground storey), are designed at this stage. In the case of bridges, it is very likely that the deck and the abutments will have (due to 'non-seismic' requirements) a higher strength than that required on the basis of this analysis. A notable exception is continuity slabs in decks consisting of precast-prestressed beams with cast in situ top slab, a structure quite different from the box girder deck bridges that are the focus of this paper. Such slabs will certainly yield under this level of seismic action, but this is perfectly within the design philosophy of such bridges and is also allowed by the codes; there is no need for verification of the plastic rotation either, since the shallow sections of R/C slabs can develop very high rotations without rupture; deck slab hinging can readily be addressed within the proposed procedure (by adding the pertinent hinges in the PIM), but this case is not studied herein. Deformation limit-states for yielding elements (i.e. the piers) can be computed as in the previous step by adopting relevant material strains (e.g. Kowalsky 2000); however, it will be seen (see Section 3) that deformation demand is not critical at this PL apart from the case when a hazard level higher than the one corresponding to bridges of average importance in EC8-2 is adopted. On the contrary, it is essential that bearing deformations be checked at this stage; allowable strain values for typical elastomeric bearings can be set to around 2.0, which corresponds to the yielding of steel shims (Mori *et al.* 1997). The latter value is also adopted by EC8-2.

Step 4 – Design for shear: To account for the less ductile nature of this mode of failure, shear forces should be calculated for seismic actions corresponding to a higher level of intensity (denoted as EQIV and often associated with a T_r of 2500 yrs), for which the 'collapse-prevention' PL is verified. However, to simplify the design procedure, design and detailing for shear can be carried out using shear forces calculated from inelastic response-history analysis for the seismic action associated with the 'life-safety' PL, and implicitly relate them to those corresponding to the 2%/50yr earthquake through appropriately selected magnification factors (γ_v). Recommended γ_v factors, accounting mainly for the strain-hardening effect (Section 3.2) corresponding to higher plastic rotations at this earthquake level, are between 1.10 and 1.20.

Step 5 – Detailing of critical members: Detailing of R/C piers for confinement, anchorages and lap splices, is carried out with due consideration of the expected level of inelasticity. Detailing of piers can be carried out according to the provisions of EC8-2 for ductile members. However, instead of basing the detailing on the default curvature ductilities specified in the Code (μ_φ=13 for bridges of ductile behaviour), the actual μ_φ estimated for the earthquake associated with the 'collapse-prevention' requirement are used in this PBD method. This results in both more rational and, as a rule, more economic, detailing of the piers. Moreover, it should be verified that bearings do not exceed their ultimate deformability; in the case of usual elastomeric bearings, although it is well known that under shear loading the shear strain at failure can exceed 400% (Konstantinidis *et al.* 2008, Moschonas *et al.* 2009), stability considerations are expected to yield the critical (i.e.

allowable) shear strain limit under the 'collapse-prevention' earthquake level.

3. Evaluation of the proposed procedure in the case of an existing bridge

3.1 Description of studied bridge

The selected structure (Overpass T7 in Egnatia Motorway, see Fig. 2), is of a type common in modern motorway construction in Europe. The 3-span structure of total length equal to 99 m is characterized by a significant longitudinal slope (approximately 7%) of the 10 m wide prestressed concrete box girder deck that results in two single column piers (cylindrical cross section) of unequal height (clear height of 5.9 and 7.9 m). The deck is monolithically connected to the piers, while it rests on its abutments through elastomeric bearings; movement in both directions is initially allowed at the abutments, while longitudinal and transverse displacements are restrained whenever a 10 and a 15 cm gap (between the deck and the abutment) is closed, respectively. The bridge rests on firm soil and the piers and abutments are supported on surface foundations (footings) of similar configuration. The above geometrical characteristics (i.e. different pier heights and unrestrained response of the deck at the abutments) result in an increased contribution of the second mode, rendering the specific bridge an interesting benchmark for the evaluation of design and/or assessment methodologies (e.g. Paraskeva *et al.* 2006). In fact, as mentioned earlier, a key consideration in the selection of the studied bridge was the possibility to compare the design results derived from two alternative PBD methods, the Def-BD procedure proposed herein, and the MDDBD procedure (Kappos *et al.* 2013); hence for the sake of consistency, certain design parameters were defined in line with the latter study.

The EC8 'Type 1' elastic spectrum (T_r=475 yrs) for two different seismic hazard zones (i.e. Zone II: PGA of 0.21g, Zone III: PGA of 0.31g) was the basis for seismic design (i.e. EQIII in Table 1), corresponding to subsoil class 'C' of the Code. However, a significant modification compared to the EC8 elastic response spectrum was made; a corner period (i.e. the value defining the beginning of the constant displacement response range of the spectrum) equal to 4.0s was adopted (instead of 2.0s, the EC8 recommended value). This modification, apart from being in line with recent research findings (e.g. Priestley *et al*. 2007), was initially adopted in Kappos *et al*. (2013) as necessary for the MDDBD to be meaningful in the sense that short corner periods lead to small displacement values in the period range that is common to direct displacement-based design method (which involves secant stiffness values at maximum displacement).

In the analyses presented in the following, the focus is on the transverse response of the bridge. Although this was done for the sake of consistency with the MDDBD study, it should be understood that the Def-BD methodology presented herein can inherently account for the response in both principal directions of the structure, and in fact for seismic actions applied simultaneously in both directions (Kappos and Stefanidou 2010). In applying the Def-BD procedure to this bridge, the gap size and the characteristics of the bearings are treated as design parameters; i.e. activation of the abutment-backfill was not considered, whereas the output of the MDDBD methodology regarding the geometry of the piers (i.e. D=1.5m) and the mechanical characteristics of the bearings (plan dimensions of 350×450mm with total thickness of elastomer t_r=88mm) was used as a starting point. The bridge was designed as a ductile structure, accounting for the effect of geometric nonlinearities (P-Δ analysis), while ignoring soil-structure interaction phenomena (similarly to Kappos *et al.* 2013). Analysis was carried out using Ruaumoko 3D software (Carr 2006), while SAP2000 (CSI 2009) was also used for additional verification; further information regarding the bridge configuration and modelling can be found in Kappos *et al.* (2013).

Fig. 2 Overpass T7, Egnatia Motorway, N. Greece (Google Earth 2011)

3.2 Application of the procedure

Step 1: A standard RSA was first performed to provide the strength of the members (energy dissipation zones) that are expected to respond inelastically under an earthquake with a high probability of exceedance, considered as 40% in 50 years according to the performance objective adopted herein (see Table 1). The earthquake associated with the 'operationality' PL was taken as 1/2 of the Eurocode design spectrum (corresponding to EQIII) along the lines suggested in EC8 for serviceability checks. The reduction factor v_0 related to the required performance of the structure under the selected earthquake level (see Section 2) was taken equal to 0.75.

Pier stiffness was estimated on the basis of yield condition in the pier by taking into account the effects of axial load ratio as proposed by Priestley *et al.* (1996) and ATC-32 (ATC 1996), considering axial load from service loading, and assuming a minimum ρ_l of 1%. An effective flexural stiffness equal to 43% and 39% of the gross section was obtained for pier columns in Zones II and III, respectively (different diameter is used in each zone, see next steps). The superstructure was assumed to respond essentially elastically, as far as its flexural stiffness is concerned, while its torsional stiffness was set equal to 20% of the uncracked section torsional stiffness (Katsaras *et al.* 2009), assuming cracking due to torsion.

Table 1 Selected performance objectives

PE (%) in 50/100/200 yrs			T_r (yrs)	Earth-quake level	Full service		Limited service	Disruption of service
					Negligible damage	Minimal damage	Moderate damage	Severe damage
50	100	200			No repair	Minimal repair	Feasible repair	Replacement**
*	*	*	*	EQI	●			
40.9	65.1	87.8	95	EQII		●		
10.0	19.0	34.4	475	EQIII			●	
2.0	4.0	7.8	2462	EQIV				●

* Implicit definition according to Step 1

** Partial or complete replacement may be required

The strength of the selected dissipation zones (i.e. the base and top of pier columns) was estimated taking into consideration the range within which the inelastic deformations should fall, which corresponds to the degree of damage allowed for the 'operationality' PL (associated with EQII in 'typical' bridges). It should be noted that allowable rotational ductility factors considered at this stage of design were approximately calculated according to Eqs. (1) to (3). The allowable rotational ductility factors were estimated according to Eq. (1), where the index '*ls'* indicates a limit-state deformation or ductility factor associated with the specific PL (i.e. EQII at this stage). Assuming a 'serviceability'-related concrete strain between 3.5 and 4.0‰, φ_{ls} was derived from relevant charts, proposed by Kowalsky (2000), whereas φ_y and L_{pl} were obtained from Eqs. (2) and (3) respectively (Priestley *et al*. 2007); the same equations were used in Kappos *et al.* (2013). The equivalent cantilever height was estimated from the results of the RSA (see Table 3). Updated and more accurate values of strains, curvatures, chord rotations and ductility factors corresponding to specific PLs were computed at Step 2. Finally, the allowable strain of the bearings under the specific PL was assumed equal to 1.0 (see Section 2).

$$\varphi_y = 2.25 \cdot \varepsilon_y / D \tag{2}$$

$$L_{pl} = k \cdot h_{eq} + 0.022 \cdot f_y \cdot \varnothing_L, \;\; k = 0.2 \cdot \left(\frac{f_u}{f_y} - 1 \right) \leq 0.08 \tag{3}$$

Elastic chord rotations (θ_{el}) were related to the corresponding inelastic ones (θ_{inel}), using an empirical modification factor of 1.22 as proposed by Bardakis and Fardis (2011). Following the design process described in Section 2, $\mu_{\theta,ls}$ were found equal to 1.65 and 1.55 for pier 1 (P_1) and pier 2 (P_2) respectively for Zone II design, and 1.58 and 1.48 for Zone III. Referring to the case of Fig. 1(a), the corresponding yield moments were defined as the intersection of the elastic part of the diagram and the vertical line drawn at $\theta_y = \theta_{inel}/\mu_{\theta,ls}$. It is noted here that the reduced design moments calculated according to the aforementioned procedure are implicitly related to the flexural demand under the EQI PL (see Table 1) that correspond to the yield state of the structure. The more accurate procedure described in Section 2 for defining the pier design moments (Fig. 1(b)) was not used since the pertinent combination of permanent and transient actions does not affect the transverse response of the bridge, considered herein.

Using standard design aids for flexure with axial loading and design values for strength of materials, Step 1 yielded in the case of Zone II a ρ_l of 10.4 ‰ for each pier column, with a 1.2 m diameter (M-θ response is given in Fig. 5 as the 'D-L-RSA' case). It is worth noting that a 1.5 m diameter was considered as a starting point for the case of Zone II, corresponding to the design output of the MDDBD method (i.e. D=1.50 m, $\rho_{l,P1}$=9.8‰, $\rho_{l,P2}$=12.4‰). However, since ρ_l demand was found less than 1% (actually it was found less than 0.5%) and the shear strain of the elastomeric bearings was less than 100%, the diameter was gradually reduced to 1.2 m (resulting design quantities can be found in Table 3 under the 'EQII-D-L' case). Likewise, for Zone III, wherein a 1.7 m diameter was selected, the design process yielded ratios of $\rho_{l,P1}$=12.5‰ and $\rho_{l,P2}$=9.5‰, accompanied by a minor exceedance (i.e. 7%) of the bearing strain limit at the right abutment (Abt_2) (larger diameter of pier columns resulted in substantially lower ρ_l); it is noted that D=2.0 m, $\rho_{l,P1}$=11.5‰, $\rho_{l,P2}$=19.0‰ were the corresponding design results in the case of MDDBD.

Step 2: Selection of 'structure-specific' input ground motions for response-history analysis was made using the ISSARS software (Katsanos and Sextos 2013) that utilizes the Next Generation Attenuation Strong-Motion database, PEER-NGA (Chiou *et al.* 2008). In the case of Zone II, 18

eligible pairs of seismic events were initially selected by adopting as preliminary search criteria a magnitude M_s=6.0-7.0, an epicentral distance R=10-25 km, site class 'D' according to the NEHRP provisions (FEMA 2009) (equivalent to subsoil class 'C' of EC8-1), and a PGA of 0.21-0.42g. It is noted that values of PGA were set in the previous range as a means to select ground motions with acceleration ordinates that would yield scaling factors close to unity for the EQIII level. Subsequently, utilising the scaling procedure adopted by EC8-1 the selected accelerograms were used as seed motions to form 31824 eligible suites of seven records ranked according to the similarity of spectra (those of the selected motions to the EQIII target spectrum), as quantified by the normalised root-mean-square-error (δ) (Katsanos and Sextos 2013). The selection of the suite of records adopted in the present design (see Table 2) was additionally based on a maximum accepted variability in the pier displacements. To this effect, a threshold value of the standard error of estimate (SEE) equal to 15% was adopted (assuming a two-sided Student-t probability density function and 90% confidence level). Calculated SEEs were based on the results obtained from linear RHA of the bridge under the 18 eligible events. Although a more refined approach would require a ground motion selection based on different criteria (e.g. higher values of magnitude and PGA) in the case of Zone III, the same eligible pairs of seismic events were adopted herein for the sake of simplicity, and with a view to investigating how the final design is affected by a higher earthquake level, disengaged from parameters associated with the variability of preliminary selection criteria; this inevitably led to scaling factors higher than 1 for Zone III (Table 2).

It is noted that since only the transverse response of the bridge is considered herein, the mean spectrum was scaled so that it was not lower than 0.9 times the modified (i.e. corner period equal to 4.0s) EC8 5%-damped elastic response spectrum for ground C within the period range $0.2T_1$~$1.5T_1$, yielding the scaling factors of Table 2; implementation of the EC8-2 scaling procedure within the same period range, wherein the ensemble 5% damping elastic spectrum calculated from the SRSS spectra of all time histories is compared with 1.3 times the EC8 spectrum, results in practically the same values of scaling factors). The above scaling procedure resulted in the spectral matching depicted in Fig. 3 for the second set of horizontal components (HC2) (although the normalized error (δ) was found lower in the case of the HC1 set, HC2 was finally adopted as the seismic input in subsequent steps, due to the superiority of this particular set with regard to the established confidence level of structural response (i.e. lower SEE)).

A PIM of the structure was set up; the columns of the piers (top and bottom) were modelled as yielding elements, while the remaining parts (i.e. deck, bearings, foundations) were modelled as elastic members. Assuming a code minimum transverse mechanical reinforcement ratio ($\omega_{w,min}$=0.18 herein, according to EC8-2), the strength and the effective stiffness of the dissipating zones (based on mean values for material properties and the ratio ρ_l computed in Step 1) were defined through M-φ analysis utilising the computer program RCCOLA.NET (http://83.212.120.208/vlabs/ Methodology.aspx). Refined deformation limits (i.e. curvatures and curvature ductility factors) based on allowable strains associated with the 'operationality' (i.e. $\varepsilon_{c,ls}$=3.5-4‰ or $\varepsilon_{s,ls}$=15‰) and the 'damage- limitation' PLs (i.e. $\varepsilon_{c,ls}$=18‰ and/or $\varepsilon_{s,ls}$=60‰) (Kowalsky 2000), were also calculated in this step. Further information regarding the modelling of hysteretic behaviour in Ruaumoko 3D (Carr 2006) can be found in Kappos *et al.* (2013).

Table 2 Selected ground motions and suites of records

No.	Name	Region	Date	Station	Magnitude	Distance (km)	PGA(g)	Hor. Component 1 (HC1)	Hor. Component 2 (HC2)
1	Imperial Valley-02	USA	19.05.1940	El Centro Array #9	6.95	12.99	0.258	IMPVALL_I-ELC180	IMPVALL_I-ELC270
3	Imperial Valley-06	USA	15.10.1979	Chihuahua	6.53	18.88	0.270	IMPVALL_H-CHI012	IMPVALL_H-CHI282
5	Imperial Valley-06	USA	15.10.1979	Holtville Post Office	6.53	19.81	0.248	IMPVALL_H-HVP225	IMPVALL_H-HVP315
6	Imperial Valley-06	USA	15.10.1979	SAHOP Casa Flores	6.53	12.43	0.357	IMPVALL_H-SHP000	IMPVALL_H-SHP270
8	Corinth, Greece	Greece	24.02.1981	Corinth	6.60	19.92	0.264	CORINTH_COR--L	CORINTH_COR--T
10	Northridge-01	USA	17.01.1994	Arleta - Nordhoff Fire St.	6.69	11.10	0.330	NORTHR_ARL090	NORTHR_ARL360
12	Northridge-01	USA	17.01.1994	LA - Hollywood Stor FF	6.69	23.61	0.335	NORTHR_PEL090	NORTHR_PEL360
13	Northridge-01	USA	17.01.1994	LA - N Faring Rd	6.69	16.99	0.246	NORTHR_FAR000	NORTHR_FAR090
16	Kobe, Japan	Japan	16.01.1995	Kakogawa	6.90	24.20	0.267	KOBE_KAK000	KOBE_KAK090

Zone	Suite of records							Scaling factor (SF)	Spectral deviation δ	P_1 SEE (%)	P_2 SEE (%)
II	1	3	5	6	12	13	16	1.18	0.1651	13.17	13.51
III	1	5	6	8	10	13	16	1.81	0.1956	12.33	14.74

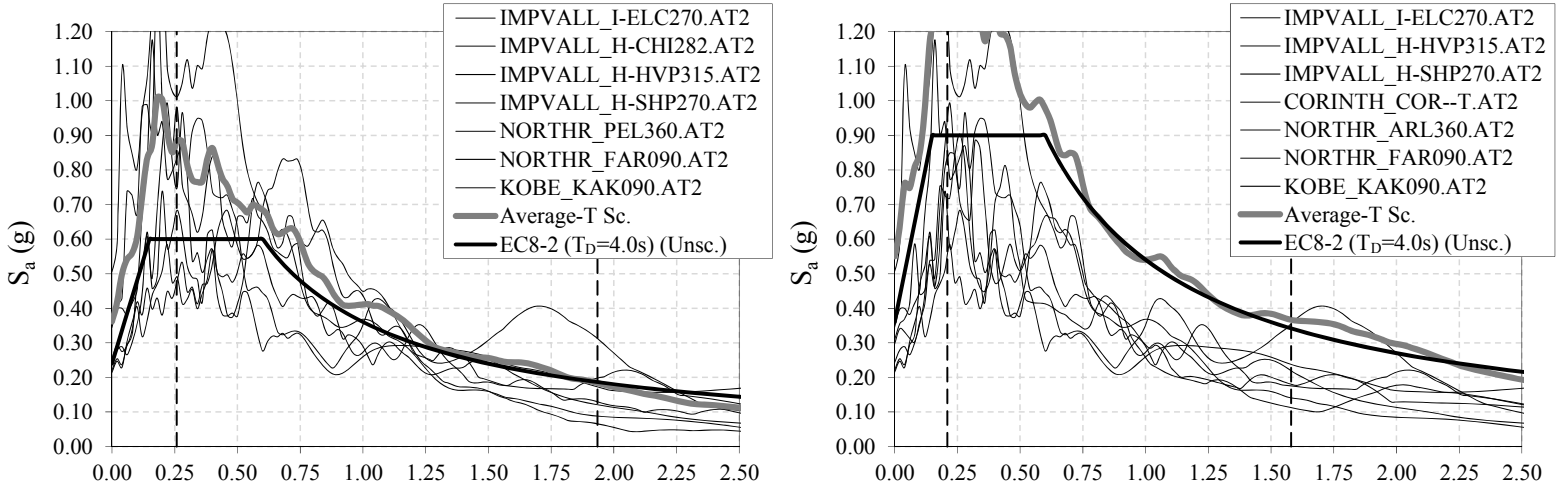

(a) Zone II (PGA=0.21g) (b) Zone III (PGA=0.31g)

Fig. 3 Spectral matching of the Horizontal Component 2 scaled average response spectrum to the target spectrum

Inelastic dynamic analyses of the bridge were performed under the suite of records of Table 2 (bottom) scaled to the intensity corresponding to EQII. 'Operationality' verifications included specific limits for maximum curvature and chord rotation ductility factors in the case of pier columns, and specific strain limits in the case of elastomeric bearings (shear strain limit of 1.0 was adopted for EQII). Limit-state chord rotation ductility factors were computed based on the refined yield curvatures and 'damage-based' curvatures (resulting from the M-φ analysis), and the estimation of the equivalent cantilever height for the piers according to the results of the NLRHA; the latter were calculated as the average of the span ratios observed in the pier-columns during the 7 RHAs at the time step each member enters the inelastic range (i.e. when the bending moment at the critical section first reaches the yield moment). Key results are provided after the following step.

Step 3: Inelastic dynamic analyses were run for the same accelerograms, now scaled to the EQIII level. 'Repairable damage' verifications also included limits for maximum curvature and chord rotation ductility factors in the case of pier columns, and strain limits in the case of the elastomeric bearings; for this check, a shear strain limit of 2.0 was adopted for the bearings. EC8-2 imposes the same deformation limit (i.e. 2.0) on the maximum total design strain under the 'design earthquake' (EQIII) which is associated with the combined effect of seismic design displacements (d_E) (including effects of torsional response around a vertical axis), long-term displacements due to the permanent and quasi-permanent actions (d_G) (e.g. prestressing after losses, shrinkage, creep), and displacements due to thermal actions (d_T). Nevertheless, its adoption exclusively for the seismic design displacement should not be deemed incompatible since in the transverse direction, considered herein, d_G and d_T are equal to zero, while the value of d_E at the level of the deck soffit does not include a contribution from the rotation of the end section of the deck.

The displacement demand profiles obtained through the different stages of design (denoted as D) are illustrated in Fig. 4, whereas in Fig. 5 chord rotation demands resulting from the design procedure (RHA) are compared with the target-deformations (SA, for 'Section Analysis', used to derive the limit-state deformations). Further design quantities (i.e. effective stiffnesses, curvature and displacement ductility factors, column drifts, pier equivalent cantilever heights and elastomeric bearing strains) are presented in the companion Table 3. Displacements and deformations presented in the aforementioned figure and table as the nonlinear case (NL) are the average of the quantities recorded in the structure during the 7 RHAs, either at the time step each member enters the inelastic range or at the time step of maximum response.

It is evident that the performance criteria associated with the 'operationality' PL control the design while excellent agreement is found between target-deformation quantities and design quantities resulting from NLRHA; clearly this is mainly due to the consistent assumptions made for pier stiffness. In the case of Zone II, further reduction of the column diameter aiming at bringing the demand closer to the deformation limit at the location of Abt_2 would render critical the design under the pertinent combination of permanent and transient actions. A slight exceedance of the target-deformations under EQII is observed at the base of P_1 (see Fig. 5); however, since the relevant curvature (or chord rotation) corresponds to a compressive concrete strain that is equal to 4‰ (i.e. within the range of accepted values in the literature), it was deemed appropriate to proceed the design to the next step without increasing ρ_l. With regard to the performance of P_2 (for Zones II & III), a decrease of the ρ_l ratio (that would result in improved convergence) was omitted due to minimum requirements (i.e. ~1%).

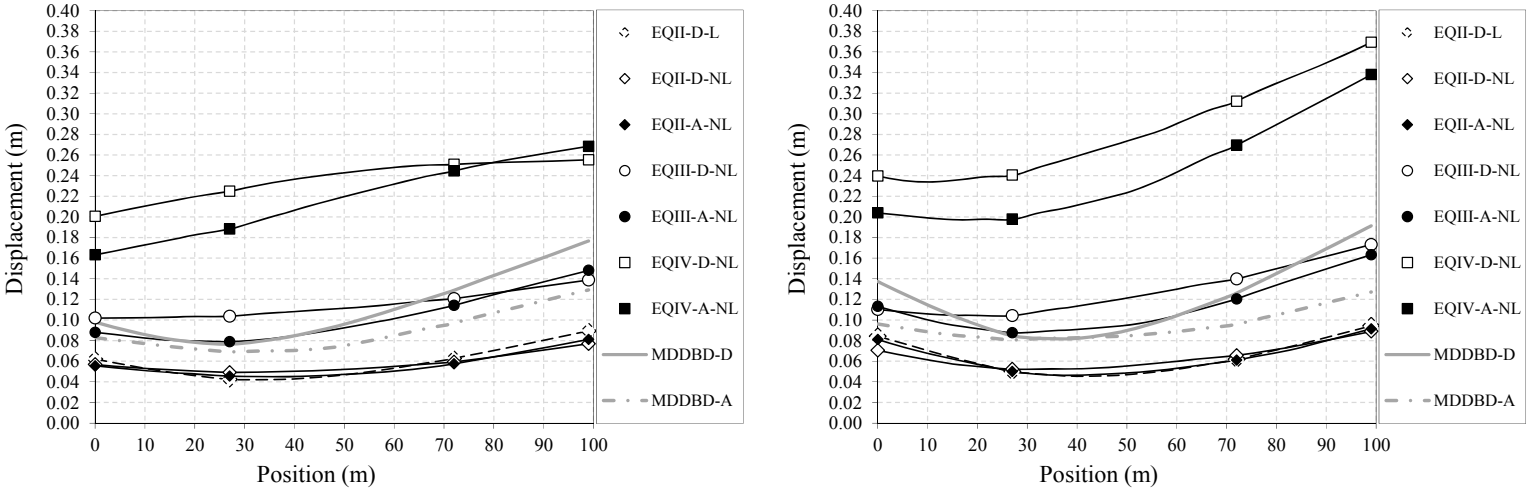

(a) Zone II (PGA=0.21g) (b) Zone III (PGA=0.31g)

Fig. 4 Response spectrum (L) and nonlinear response history (NL) maximum displacement demands, derived from design (D) and assessment (A) under EQII, EQIII and EQIV, also compared with the MDDBD design (D) and assessment (A) displacements

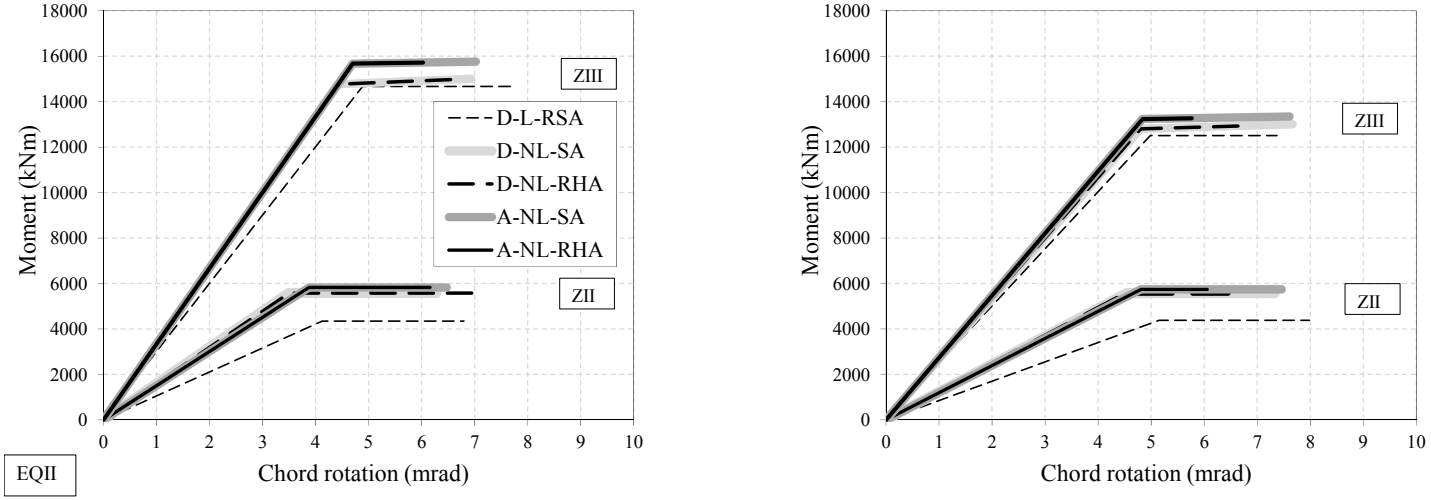

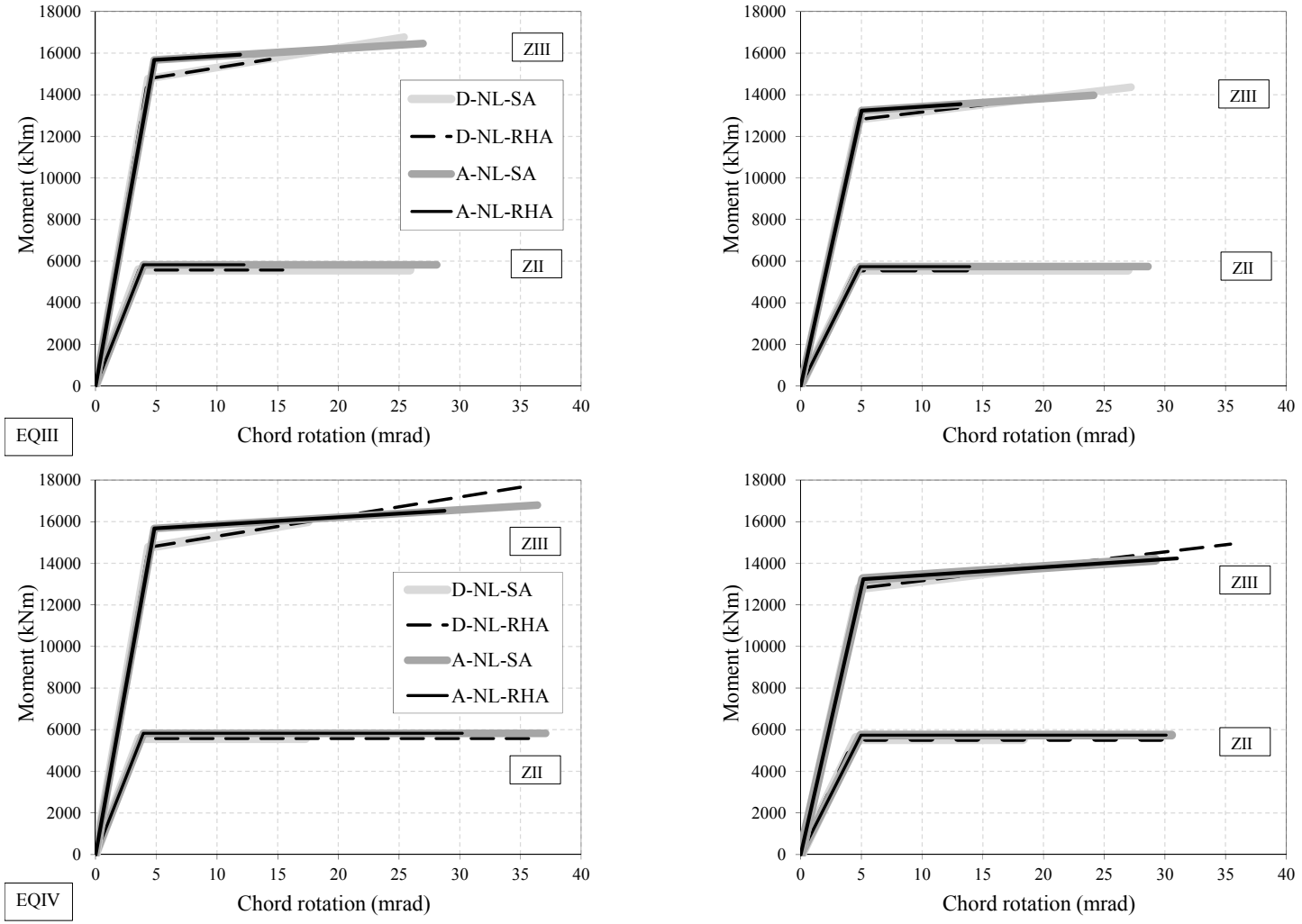

(a) Pier 1 (b) Pier 2

Fig. 5 Moment-chord rotation demand curves (RSA, RHA) derived from design (D) and assessment (A) in the case of Zone II & III, under EQII, EQIII & EQIV at the base of the pier columns, compared with allowable limit-state deformations (SA)

Table 3 Design quantities for Zones II & III

Case		Zone II										Zone III									
		EQII-D-L	EQII-D-NL		EQII-A-NL		EQII-D-L	EQII-D-NL		EQII-A-NL		EQII-D-L	EQII-D-NL		EQII-A-NL		EQII-D-L	EQII-D-NL		EQII-A-NL	
			SA	RHA	SA	RHA		SA	RHA	SA	RHA		SA	RHA	SA	RHA		SA	RHA	SA	RHA
Member		Column 1					Column 2					Column 1					Column 2				
EI_y/EI_g (%)	Base	43.0	65.9		61.0		43.0	65.8		62.1		39.0	43.4		40.8		39.0	42.5		40.7	
	Top	43.0	65.9		61.0		43.0	65.8		62.1		39.0	43.4		40.8		39.0	42.5		40.7	
μ_φ	Base	2.31	2.72	3.17	2.43	2.25	2.31	2.73	2.19	2.51	1.71	2.49	2.56	2.42	2.28	1.73	2.49	3.01	2.29	2.80	1.60
	Top	-	2.76	0.71	2.46	0.65	-	2.77	0.71	2.55	0.71	-	2.61	0.32	2.32	0.34	-	3.11	0.47	2.88	0.48
$\mu_{\theta,ch}$	Base	1.65	1.79	2.00	1.67	1.59	1.55	1.62	1.42	1.55	1.26	1.58	1.57	1.52	1.49	1.28	1.48	1.60	1.39	1.57	1.19
	Top	-	2.08	0.71	1.89	0.65	-	1.81	0.71	1.71	0.71	-	2.03	0.32	1.83	0.34	-	2.01	0.47	1.89	0.48
μ_Δ		-	-	1.70	-	1.46	-	-	1.25	-	1.17	-	-	1.42	-	1.26	-	-	1.30	-	1.18
Drift (%)		-	-	0.68	-	0.63	-	-	0.64	-	0.62	-	-	0.72	-	0.69	-	-	0.71	-	0.66
h_{eq} (m)	Base	3.69	-	3.94	-	3.87	4.66	-	5.11	-	4.95	4.65	-	4.98	-	4.70	5.67	-	6.12	-	5.71
	Top	2.25	-	2.96	-	2.97	3.27	-	3.95	-	3.96	1.29	-	2.84	-	2.89	2.26	-	3.78	-	3.85
Member		Abutment 1					Abutment 2					Abutment 1					Abutment 2				
γ%		70.5	100.0	64.6	100.0	63.2	101.5	100.0	87.5	100.0	92.2	95.9	100.0	80.2	100.0	92.2	107.2	100.0	101.1	100.0	104.0
Case			EQIII-D-NL		EQIII-A-NL			EQIII-D-NL		EQIII-A-NL			EQIII-D-NL		EQIII-A-NL			EQIII-D-NL		EQIII-A-NL	
			SA	RHA	SA	RHA		SA	RHA	SA	RHA		SA	RHA	SA	RHA		SA	RHA	SA	RHA
Member		Column 1					Column 2					Column 1					Column 2				
μ_φ	Base		14.85	9.00	14.28	5.55		14.86	7.24	14.47	6.12		14.11	7.17	13.20	4.89		16.77	8.38	13.44	6.28
	Top		15.04	4.02	14.48	1.40		15.18	3.22	14.74	2.16		14.35	0.59	13.43	0.52		17.25	0.95	13.85	0.78
$\mu_{\theta,ch}$	Base		7.26	4.62	7.10	3.09		5.87	3.19	5.83	2.84		5.89	3.33	5.58	2.46		5.76	3.24	4.81	2.63
	Top		9.62	2.85	9.25	1.23		7.51	1.98	7.31	1.53		9.53	0.59	8.81	0.52		8.76	0.90	7.06	0.78
μ_Δ			-	3.51	-	2.44		-	2.54	-	2.22		-	2.89	-	2.13		-	2.77	-	2.24
Col. Drift (%)			-	1.43	-	1.09		-	1.30	-	1.23		-	1.43	-	1.21		-	1.51	-	1.30
h_{eq} (m)	Base		-	4.02	-	3.95		-	5.17	-	5.06		-	4.86	-	4.83		-	6.02	-	5.92
	Top		-	2.96	-	2.97		-	3.95	-	3.96		-	2.84	-	2.89		-	3.80	-	3.85
Member		Abutment 1					Abutment 2					Abutment 1					Abutment 2				
γ%			200.0	115.8	200.0	100.2		200.0	157.8	200.0	168.3		200.0	125.3	200.0	128.6		200.0	196.9	200.0	185.6
Case			EQIV-D-NL		EQIV-A-NL			EQIV-D-NL		EQIV-A-NL			EQIV-D-NL		EQIV-A-NL			EQIV-D-NL		EQIV-A-NL	
			SA	RHA	SA	RHA		SA	RHA	SA	RHA		SA	RHA	SA	RHA		SA	RHA	SA	RHA
Member		Column 1					Column 2					Column 1					Column 2				
μ_φ	Base		9.48	21.27	19.22	15.44		9.48	17.23	15.54	15.28		9.14	20.49	18.39	14.17		10.84	22.42	16.65	17.74
	Top		9.59	16.45	19.50	10.90		9.66	12.43	15.79	10.71		9.30	7.29	18.74	2.70		11.15	7.83	17.09	7.09
$\mu_{\theta,ch}$	Base		4.78	10.03	9.42	7.67		3.98	6.70	6.16	6.07		3.99	8.20	7.52	5.93		3.88	7.28	5.67	6.03
	Top		6.26	10.46	12.34	7.06		4.97	6.24	7.80	5.46		6.31	5.01	12.13	2.07		5.87	5.73	8.58	3.87
μ_Δ			-	7.62	-	5.72		-	5.20	-	4.67		-	6.57	-	4.82		-	6.05	-	4.88
Col. Drift (%)			-	3.09	-	2.59		-	2.71	-	2.64		-	3.31	-	2.72		-	3.37	-	2.91
h_{eq} (m)	Base		-	4.07	-	3.93		-	5.17	-	5.11		-	4.94	-	4.84		-	6.20	-	6.08
	Top		-	2.96	-	2.96		-	3.96	-	3.95		-	2.84	-	2.89		-	3.78	-	3.85
Member		Abutment 1					Abutment 2					Abutment 1					Abutment 2				
γ%			368.0	227.9	392.3	185.6		368.8	290.2	387.9	305.1		316.4	272.4	302.8	231.8		302.5	419.7	306.3	384.0

The 'life-safety' PL was not found critical in any of the cases studied herein (although the bearing strains of the Abt_2 were close to the deformation limits). In fact, pier deformation demands resulting from this PL were somewhat lower than the deformation limits corresponding to the minimum reinforcement ratio considered in Step 2 (presented in Fig. 5 and Table 3 as the EQIV-D-NL SA case). In Table 3, design quantities at the top of the pier columns are also presented; however, as expected, these are far from being critical to the design since the base reinforcement demand is also adopted at the pier top, according to the current bridge design philosophy of typical pier columns. It is also worth noting that in the case of Zone II, the underestimation of the pier strength during the linear analysis derives from the fact that the v_o factor does not account for the

increase in strength due to the effect of the increased axial load ratio (n_k). Although this indicates the need for considering lower values of v_o (i.e. the ratio f_{cd}/f_{cm} can be accounted for in cases of high n_k), minimum reinforcement requirements preclude their adoption.

Step 4: Design and detailing for shear was carried out using shear forces calculated from NLRHA for the seismic action associated with the 'life-safety' PL, and implicitly related to those corresponding to the 2%/50yr earthquake (i.e. EQIV) through appropriately selected magnification factors. In the case of Zone II, pier shear forces are not expected to increase under EQIV, due to the elasto-plastic bilinear approximation of the M-φ curves (see Fig. 5) derived from moment-curvature analysis, and the fact that piers exhibit inelastic behaviour at both ends (i.e. base and top) under EQIII; however, a magnification factor (γ_v) of 1.10 was applied to account for the increase in flexural strength due to the expected increase of the transverse reinforcement ratio (ρ_w) associated with the shear and confinement requirements of Steps 4 and 5 (recall that a minimum ρ_w was assumed in Step 2). Regarding Zone III, a factor of 1.20 was used to account for the strain-hardening effect (see Fig. 5). Shear design for the two seismic zones was performed according to the EC8-2 provisions using design values for material properties and assuming γ_{bd}=1 (i.e. safety factor against brittle failure); the transverse reinforcement was found to be governed by the confinement requirements of the next step, apart from the case of P_1 in Zone III.

Step 5: Detailing of piers for confinement was carried out with due consideration of the expected level of inelasticity (quantified by μ_φ) under the earthquake associated with 'collapse-prevention' PL. A magnification factor (γ_ω) equal to 2.0 was used to implicitly relate the curvature ductility demands derived from Step 3 to those expected under EQIV hazard level. Using the yield curvatures calculated in Step 2, the expected curvatures associated with EQIV were defined as $\varphi_{u,EQIV}=\mu_{\varphi,EQIV}\cdot\varphi_y$ and subsequently associated with anticipated ultimate concrete strains ($\varepsilon_{cc,u}$) according to the M-φ analysis results of Step 2. The required ρ_w were then easily obtained as a function of the ultimate concrete strains in accordance with the stress-strain model adopted in Step 2 (Kappos 1991). The above procedures (Steps 4, 5) yielded ratios of $\rho_{w,P1}$=12.4‰, $\rho_{w,P2}$=10.6‰, and $\rho_{w,P1}$=13.2‰, $\rho_{w,P2}$=10.4‰ for Zones II and III, respectively; the relevant volumetric ratios in the case of MDDBD, calculated in accordance with capacity design principles of EC8-2, were $\rho_{w,P1}$=9.1‰, $\rho_{w,P2}$=7.9‰ and $\rho_{w,P1}=\rho_{w,P2}$=10.4‰, governed by shear design.

It is noted that the same magnification factor (γ_ω) was also used to check that the bearings do not exceed their ultimate deformability based on stability criteria according to Eq. (4) (Constantinou *et al.* 2011):

$$N'_{cr}=\frac{\pi\cdot\sqrt{\lambda}\cdot G\cdot S\cdot r'}{t_r}\cdot A_r \tag{4}$$

In the empirical Eq. (4), N'_{cr} is the buckling load of a bolted bearing subjected to combined compression and lateral deformation, λ depends on the assumption for the value of the rotational modulus of the elastomeric bearing (λ=2.25 for rectangular or square bearings), G is the nominal shear modulus of the elastomer, S is the shape factor of the bearing, r' is the radius of gyration of the bonded area of the elastomer ($r^2=I'/A'$, where I' is the moment of inertia and A' the effective plan area of the bearing, i.e. area of the steel reinforcing plates), A_r is the reduced bonded area defined as the overlap between the top and bottom bonded elastomer areas of the laterally deformed bearing, and t_r is the total thickness of the elastomer. Considering the transverse response of the rectangular bearing (details of the bearings can be found in Kappos *et al.* 2013) mounted with the longer side parallel to the transverse direction of the bridge (to minimise the

rotational restraint in the longitudinal direction) and equating the buckling load with the axial load of the bearing under EQIII implicitly related to EQIV by a magnification factor of 1.30 (similar factors within the range of 1.0~1.5 were proposed by Constantinou *et al.* 2011), the previous relationship was re-ordered to derive the ultimate bearing strain (Table 3), that was in turn compared with the bearing strains recorded under EQIII multiplied by γ_ω=2.0. It is noted that Eq. (4) is also adopted by EN1337-3 (CEN 2005b) to check the buckling stability of bearings under the 'design earthquake', incorporating a safety factor of about 2 (for rectangular bearings). It is clear that in the case of Zone III (see Table 3), 'collapse-prevention' is the critical PL given the exceedance of the deformation limit observed at the location of the right abutment under EQIV; ideally, a designer should opt for an upgrade of the elastomeric bearings since an increase of the column diameter would penalize (in terms of cost) the design of piers under EQII, III (i.e. adoption of minimum reinforcement ratios). Herein, the above solution is not adopted for the sake of consistency in the design results of the different considered methodologies; it is reminded that the bearings of the right abutment are the critical elements (i.e. govern the design) in both approaches.

Although not required by the suggested procedure (see Section 2), for the sake of completeness the seismic demand deriving from explicitly considering the effects of the 2%/50yr earthquake is presented in Fig. 5 and Table 3 (EQIV-D case); these values were determined assuming that EQIV is characterized by twice the spectrum of EQIII, which is a rather conservative assumption (1.6~1.9 the design spectrum according to EC8). From the design quantities summarised in Table 3, it is evident that in most cases the pier ductilities resulting from EQIV-D are higher than the demand implicitly associated with the 'collapse-prevention' PL by magnification factors, indicating that an explicit consideration of the latter PL simply by magnifying the ground motions associated with EQIII leads to a more conservative design. The previous remark simply points to the fact that the calibration of magnifications factors was based on assessment procedures accounting for the final design configuration of the structural elements (e.g. modification of yield properties attributed to final detailing and increased transverse reinforcement), using artificial records closely matching the design spectrum (considering that the uncertainty related to the input motion is incorporated in the definition of the uniform hazard spectrum prescribed by the Code), and resulting in general to a safe design (see next section). Attention should be also drawn to the fact that the deformation limit violation observed in Fig. 5 does not affect the reliability of the methodology since at this stage of design the SA curves reflect the capacity of the minimum ρ_w assumed at Step 2.

3.3 Assessment of the deformation-based design procedure

Assessment of the design presented in the previous section was carried out in order to evaluate the efficiency of the proposed design procedure for the three different PLs, i.e. 'operationality', 'repairable damage' and 'collapse-prevention'. Since the primary objective of the assessment was the study of the transverse response of the bridge under a seismic excitation that matches as closely as feasible the 'design excitation' (i.e. the design spectrum), NLRHAs were performed for each design case (Zone II, III), using 5 artificial records (identical to those used to assess the MDDBD approach in Kappos *et al*. 2013), generated with the computer program ASING (Sextos *et al*. 2003) to fit the elastic design S_a spectra associated with the 'repairable damage' PL, and scaled appropriately when a different PL was considered. *M*-φ analyses based on mean values for material properties and the final detailing of reinforcement according to the results of Section 3.2 were performed for each pier section utilizing the computer program RCCOLA.NET; updated

limit-state deformations and ductility factors based on allowable material strains were recalculated. The assessment focused mainly on whether the design quantities recorded in critical members of the bridge are close to those assumed at the design stage and whether the design can be deemed as safe with respect to the refined limit-state ductility factors.

In Fig. 4 (Section 3.2) the displacement envelopes derived from the assessment procedure (denoted as A) are compared with those computed during the design (D); the deck displacements shown in the figure as case (A) are again the average of the maximum displacements recorded in the structure during the five RHAs. Fig. 5 (supplemented by Table 3) illustrates the correlation in the design quantities of interest between design and assessment, in the case of Zones II and III. An overall agreement of deformation demand can be observed between design and assessment, more so in the case of EQII, where the pier columns enter the inelastic range without exhibiting large deformations (as dictated by the PL requirements). The main difference between design and assessment quantities is noted in the area of Abt_1 and P_1 under EQIV, with differences decreasing in the area of P_2 and Abt_2. These differences should be attributed to the fact that the structure-specific earthquake ground motion selection (Step 2) was based on pier displacements obtained from linear RHAs of the bridge structure; therefore, as the members exhibit larger inelastic deformation (hence modifying the dynamic characteristics of the initially elastic structure), SEE is increased, which in turn reduces the confidence level of the mean structural response. Although use of nonlinear RHA during the ground motion selection can overcome the previous deficiency, it inevitably involves increased computational effort.

As far as the verification of the reliability of the design procedure is concerned, the design was found to be safe, in that it satisfied the limit-state deformations associated with the relevant PLs (even in the case of EQII-Zone II where a slight exceedance of the deformation limit was observed during design at the base of P_1), since the deformation demand derived from the assessment procedure was in general lower that the one derived at the design stage. Only in the case of the 'collapse-prevention' PL (under EQIV) a minor exceedance of the deformation capacity (~6%) is recorded at the base of P_2 (Fig. 5(b), bottom diagram). Similar conclusions are drawn with respect to the shear strength (assessed using mean values of strengths of materials), the confinement requirements and the bearing strains (the exceedance of bearing strains at Abt_2 under EQIV-Zone III was discussed in Section 3.2). On the other hand, the reduced deformation demand (compared to the relevant deformation capacity) in the EQII-Zone III assessment case, is ascribed to the bilinear approximation of the M-φ curves at the design stage (based on the equality of areas under the 'exact' and the bilinear curve) that included a post-elastic branch with a non-zero slope and thus entailed a lower (effective) M_y (deriving from the consideration of a minimum ρ_w in Step 2 that resulted in a lower ultimate curvature); in this case, a zero post-elastic slope of the M-φ curve is expected to lead to smaller discrepancy between design and assessment quantities, as in the case of Zone II). Nevertheless, in the example studied herein, the adoption of elastic-perfectly-plastic curves in Zone III would not result to a substantially different design output since an attempt to reduce ρ_l ratios during design (aiming to match more closely the deformation limits) would be obstructed by minimum reinforcement requirements.

3.4 Comparison of Def-BD with MDDBD

Despite the notable differences regarding the design principles adopted by the PBD methodologies discussed herein (i.e. Def-BD and MDDBD) with regard to the type of analysis (inelastic vs. elastic), the definition of the seismic input (set of accelerograms vs. displacement

spectrum), the type of stiffness used to control design quantities (i.e. secant stiffness at yield vs. at maximum response), the range of directly controlled parameters (e.g. displacements, deformations, strains) and the number of iterations required (Kappos 2014), both methodologies aim at a specific structural performance under a number of earthquake levels, and not surprisingly yield generally similar drifts and displacements, at least for the PL ('life-safety') for which explicit verifications were carried out in both procedures; displacement profiles derived from MDDBD and its assessment can be viewed in Fig. 4, while further design quantities can be found in Kappos *et al.* (2013). The ability of each methodology to accurately capture the structural response under a specific PL depends on the type of analysis used (along with the definition of the seismic input). Elastic RSA, forming part of MDDBD, similarly to force-based based code procedures using this analysis, attempts to capture the maximum probable response to a given seismic action (after the formation of plastic hinges) based on a statistical combination (e.g. SRSS) of the peak 'modal' responses; this analysis cannot account for the modification of the dynamic characteristics of the structure during the successive formation of plastic hinges and thus its efficiency is expected to decrease as the irregularity of the structural system is increased (e.g. overestimation of the displacements at the critical elements of the studied bridge, the elastomeric bearings at Abt_2). On the other hand, RHA in Def-BD is generally sensitive to the ground motion selection; to mitigate this effect a software tool for structure-specific selection based on linear RHA is enabled. It is clear that a selection based on nonlinear dynamic analysis would lead to a better prediction of structural response (e.g. smaller discrepancy in P_1-related quantities under EQIII-Zone II between design and assessment), but at the expense of increased computational effort, which can hardly be justified in a practical design context.

Regarding the reliability of the design, both approaches are found (via deterministic assessment procedures) to be safe in the sense of satisfying the relevant performance requirements. Still, the incorporation of advanced analysis procedures (e.g. NLRHA, refined M-φ analysis) in the case of Def-BD can bring the deformation demand closer to the pertinent limits, leading to cost reduction without jeopardizing the desired performance. In the case studied, design for Zone II resulted in reductions (compared to MDDBD) of the pier longitudinal and transverse steel quantity (weight) equal to 41.7% and 17.0%, respectively. In the case of Zone III the corresponding reductions were equal to 50.7% and 19.8%; it is reminded that the transverse reinforcement in the case of MDDBD was governed by shear (in accordance with capacity design principles) while the confinement requirements were checked based on the provisions of EC8-2. The relevant reduction of the concrete volume (in piers only) was equal to 36.0% and 27.8% for Zone II and III design, respectively. As a general remark, design in both methodologies was limited to a certain degree by the minimum ρ_l, considered herein as 1%. Following strictly the Eurocode provisions, the ratio prescribed in EC8-1 (i.e. 1%) applies only to concrete columns in buildings. Nonetheless, it is usually applied in practice by bridge designers that consider the minimum steel ratio specified in EC2 (CEN 2004a) (regarding all types of concrete columns) as insufficient for earthquake resistance. Given that the essential requirement of EC8-2 refers to a minimum local ductility of the dissipating zones, the minimum required ratio can be defined in terms of providing a strength exceeding at least the pier cracking moment; this will normally correspond to ratios of around 5‰ (Fardis *et al.* 2012), thus resulting in further cost reduction and a more reliable structural performance.

Overall, what essentially differentiates Def-BD from other PBD methods is its ability to control a broader range of design parameters (i.e. from strains up to flexural deformations and drifts) and PLs (i.e. two explicitly and two implicitly considered) within a single application of the method;

clearly, one can run MDDBD for different PLs (i.e. multiple applications of the method) but this would require at least double the computational effort, if at all feasible due to limitations related to low and moderated seismic hazard levels (Kappos *et al.* 2012).

4. Conclusions

An existing deformation-based design procedure initially proposed for seismic design of buildings was tailored herein to bridge structures, aiming at efficient structural design for multiple PLs using a 'single-run' procedure, via the control of a broad range of design parameters and the incorporation of advanced analysis tools. To this purpose, required extensions and/or modifications to the version of the method developed for buildings (Kappos and Stefanidou 2010) were presented. Key issues in this respect were the proper consideration of the intended plastic mechanism in the case of bridges under the relevant PLs (i.e. yielding of piers instead of beams), and the explicit treatment of elastomeric bearings (consideration of appropriate limit-states and verifications). Further improvements included the preliminary estimation (Step 1) of pier stiffness, strength, and expected inelastic response on a member-by-member basis, a feature that is feasible in bridges due to the smaller number of dissipating elements (compared to the generally large number of beams in buildings) and the simplification in the yield moment definition. Moreover, inelastic modelling of dissipating zones, allowable deformation limits, and confinement requirements (Steps 2, 3 and 5 of the method) were defined on the basis of refined section analysis.

The validity of the suggested procedure was then investigated by applying it to an actual bridge previously used as a case study by the authors to develop a different PBD approach, the so-called multimodal direct displacement based-design (MDDBD). The following conclusions were drawn based on deterministic assessment of the resulting T7-bridge designs, and comparison with MDDBD:

- With regard to the application of the suggested procedure, the 'operationality' PL governed the bridge design in both seismic zones considered, while exhibiting excellent agreement between target-deformation quantities and seismic demand. The 'life-safety' PL was not found to be critical, resulting in deformation demands similar to deformation limits that corresponded to minimum transverse reinforcement code requirements. Moreover, the 'collapse-prevention' PL, implicitly considered herein, imposed critical (with respect to stability) deformations at the elastomeric bearings.
- Assessment of the design by NLRHA using artificial records closely matching the relevant (for each PL) design spectrum, revealed that the suggested procedure predicted well the structural response while resulting in safe design in the sense of respecting the relevant deformation limits with only marginal exceedance locally.
- Def-DBD and MDDBD yielded in general similar drifts and displacements; however, the incorporation of advanced analysis techniques (i.e. NLRHA, section analysis) in the case of Def-BD (where a smaller column diameter was finally adopted) brought the deformation demand closer to the pertinent allowable values, leading to significant cost reduction, albeit at the expense of additional computational time and effort.
- Although the ability of each methodology to accurately predict the structural response depends on the adopted design principles, the control of various design parameters over multiple PLs and the use of powerful analysis tools render the Def-BD a rigorous methodology, applicable to

most common concrete bridge configurations without practical limitations related to the irregularity of the structural system considered; in fact the state-of-the-art in bridge design (e.g. existing software, advanced modelling techniques, soil-structure interaction phenomena, etc.) can be readily incorporated, whereas due to the adaptability of the method, different performance objectives accounting for the importance of the bridge can be met. In this context, Def-BD can be deemed as suitable for inclusion in future PBD codes.

- More work is clearly required to further investigate the effectiveness of the suggested procedure for complex bridge configurations (e.g. curved in plan bridges) and /or under challenging loading conditions (e.g. asynchronous pier excitation).

References

AASHTO (2011), *Guide Specifications for LRFD Seismic Bridge Design*, WA, US.

ATC (1996), *Improved Seismic Design Criteria for California Bridges: Provisional Recommendations*, CA, US.

ATC/MCEER (2004), *Recommended LRFD Guidelines for the Seismic Design of Highway Bridges. Part I: Specifications, Part II: Commentary and Appendices*, CA, US.

Bardakis, V.G. and Fardis, M.N (2011), "A displacement-based seismic design procedure for concrete bridges having deck integral with the piers", *B. Earthq. Eng.*, **9**(2), 537–560.

Biskinis, D. and Fardis, M.N. (2010), "Flexure-controlled ultimate deformations of members with continuous or lap-spliced bars", *Struct. Concrete*, **11**(2), 93–108.

Caltrans (California Department of Transportation) (2013), *Seismic Design Criteria*, (ver. 1.7), CA, US.

Caltrans (2014), *Bridge Memo to Designers*, CA, US.

Cardone, D. (2014), "Displacement limits and performance displacement profiles in support of direct displacement-based seismic assessment of bridges", *Earthq. Eng. Struct. D.*, **43**(8), 1239–1263.

Carr, A.J. (2006) Ruaumoko 3D: Inelastic dynamic analysis program. University of Canterbury, NZ.

CEN (Comité Européen de Normalisation) (2004a), *Eurocode 2: Design of Concrete Structures - Part 1-1: General Rules and Rules for Buildings (EN1992-1-1)*, Brussels, Belgium.

CEN (2004b), *Eurocode 8: Design of Structures for Earthquake Resistance - Part 1: General Rules, Seismic Actions and Rules for Buildings (EN1998-1),* Brussels, Belgium.

CEN (2005a), *Eurocode 8: Design of Structures for Earthquake Resistance - Part 2: Bridges (EN1998-2)*, Brussels, Belgium.

CEN (2005b), *Structural Bearings - Part 3: Elastomeric bearings (EN1337-3)*, Brussels, Belgium.

Chiou, B., Darragh, R., Gregor, N. and Silva, W. (2008), "NGA project strong-motion database", *Earthq. Spectra*, **24**(1), 23-44.

Choi, E., DesRoches, R. and Nielson, B. (2004), "Seismic fragility of typical bridges in moderate seismic zones", *Eng. Struct.*, **26**(2), 187-199.

Constantinou, M.C., Kalpakidis, I., Filiatrault, A. and Ecker Lay, R.A. (2011), *LRFD-based analysis and design procedures for bridge bearings and seismic isolators*, MCEER Report No. 11-0004, NY, US.

CSI (Computers and Structures Inc.) (2009), SAP2000: Three dimensional static and dynamic finite element analysis and design of structures, CA, US.

Fardis, M.N., Kolias, B. and Pecker, A. (2012), *Designer's Guide to Eurocode 8: Design of Bridges for Earthquake Resistance EN 1998-2*, ICE Publishing, London, UK.

FEMA (2009), *NEHRP Recommended Seismic Provisions for New Buildings and Other Structures*, WA, US.

FHWA (2006), *Seismic Retrofitting Manual for Highway Structures: Part 1 – Bridges*, NY, US.

fib (féderation internationale du béton) (2003), *Bulletin No.25: Displacement-based seismic design of reinforced concrete buildings*, Lausanne, Switzerland.

fib (2007), *Bulletin No.39: Seismic bridge design and retrofit - structural solutions*, Lausanne, Switzerland.

Google Earth 7.1.2.2041 (2011), *Greece 41°01'18.50" N, 24°41'20.66" E, elevation 268 ft, eye altitude 191 ft*, Street View, US Dept. of State Geographer 2014, [Viewed 3 November 2014].

Kappos, A.J. (1991), "Analytical prediction of the collapse earthquake for R/C buildings: Suggested methodology", *Earthq. Eng. Struct. D.*, **20**(2), 167–176.

Kappos, A.J. (1997), Partial inelastic analysis procedure for optimum capacity design of buildings, in Fajfar, P. and Krawinkler, H. (eds.) *Seismic Design Methodologies for the Next Generation of Codes*, Balkelma (CRC Press), Rotterdam, Netherlands, 229–240.

Kappos, A.J. (2015), Performance-based seismic design and assessment of bridges, in Ansal, A. (ed.) *Perspectives on European Earthquake Engineering and Seismology (Vol.2)*, Springer, (in press).

Kappos, A.J. and Manafpour, A. (2001), "Seismic design of R/C buildings with the aid of advanced analytical techniques", *Eng. Struct.*, **23**(4), 319–332.

Kappos, A.J. and Panagopoulos, G. (2004), "Performance-based seismic design of 3D R/C buildings using inelastic static and dynamic analysis procedures", *ISET J. Earthq. Tech.*, **41**(1), 141–158.

Kappos, A.J. and Stefanidou, S. (2010), "A deformation-based seismic design method for 3D R/C irregular buildings using inelastic dynamic analysis", *B. Earthq. Eng.*, **8**(4), 875–895.

Kappos, A.J., Gidaris, I.G. and Gkatzogias, K.I. (2012), "Problems associated with direct displacement-based design of concrete bridges with single-column piers, and some suggested improvements", *B. Earthq. Eng.*, **10**(4), 1237-1266.

Kappos, A.J., Gkatzogias, K.I. and Gidaris, I.G. (2013), "Extension of direct displacement-based design methodology for bridges to account for higher mode effects", *Earthq. Eng. Struct. D.*, **42**(4), 581–602.

Kappos, A.J., Goutzika, E. and Stefanidou, S. (2007) "An improved performance-based design method for 3D R/C buildings using inelastic analysis", *ECCOMAS Thematic Conference on Computational Methods in Structural Dynamics and Earthquake Engineering*, Rethymno, June.

Katsanos, E.I. and Sextos, A.G. (2013), "ISSARS: An integrated software environment for structure-specific earthquake ground motion selection", *Adv. Eng. Softw.*, **58**, 70–85.

Katsaras, C.P., Panagiotakos, T.B. and Kolias, B. (2009), "Effect of torsional stiffness of prestressed concrete box girders and uplift of abutment bearings on seismic performance of bridges", *B. Earthq. Eng.*, **7**(2), 363–375.

Konstantinidis, D., Kelly, J. and Makris, N. (2008), *Experimental investigation on the seismic response of bridge bearings*, UCB/EERC Report No. 2008/02 , CA, US.

Kowalsky, M.J. (2000), "Deformation limit states for circular reinforced concrete bridge columns", *J. Struct. Eng.*, **126**(8), 869–878.

Mori, A., Moss, P.J., Carr, A.J. and Cooke, N. (1997), "Behaviour of laminated elastomeric bearings", *Struct. Eng. Mech.*, **5**(4), 451–469.

Moschonas, I.F., Kappos, A.J., Panetsos, P. *et al*. (2008), "Seismic fragility curves for greek bridges: Methodology and case studies", *B. Earthq. Eng.*, **7**(2), 439-468.

NZTA (New Zealand Transport Agency) (2013), *Bridge Manual (SP/M/022)*, Wellington, New Zealand.

Padgett, J.E. (2007), "Seismic vulnerability assessment of retrofitted bridges using probabilistic methods", Ph.D. Dissertation, Georgia Institute of Technology, GA, US.

Paraskeva, T.S., Kappos, A.J. and Sextos, A.G. (2006), "Extension of modal pushover analysis to seismic assessment of bridges", *Earthq Eng. Struct. D.*, **35**(10), 1269-1293.

Priestley, M.J.N., Calvi, G.M. and Kowalsky, M.J. (2007), *Displacement-Based Seismic Design of Structures*, IUSS Press, Pavia, Italy.

Priestley, M.J.N., Seible, F. and Calvi, G.M. (1996), *Seismic Design and Retrofit of Bridges*, Wiley, NY, US.

Sextos, A.G., Pitilakis, K.D. and Kappos, A.J. (2003), "Inelastic dynamic analysis of RC bridges accounting for spatial variability of ground motion, site effects and soil-structure interaction phenomena. Part 1: Methodology and analytical tools", *Earthq. Eng. Struct. D.*, **32**(4), 607–627.